



Q-Bounded Maximum Directivity of Self-Resonant Antennas

This is a pre print version of the following article:

Original:

Passalacqua, L., Yepes, C., Martini, E., Maci, S. (2023). Q-Bounded Maximum Directivity of Self-Resonant Antennas. IEEE TRANSACTIONS ON ANTENNAS AND PROPAGATION, 1-1 [10.1109/TAP.2023.3324418].

Availability:

This version is available <http://hdl.handle.net/11365/1249114> since 2023-10-23T15:19:21Z

Published:

DOI:10.1109/TAP.2023.3324418

Terms of use:

Open Access

The terms and conditions for the reuse of this version of the manuscript are specified in the publishing policy. Works made available under a Creative Commons license can be used according to the terms and conditions of said license.

For all terms of use and more information see the publisher's website.

(Article begins on next page)

Q-Bounded Maximum Directivity of Self-Resonant Antennas

Laura Passalacqua, *Student Member, IEEE*, Cristina Yepes, *Member, IEEE*, Enrica Martini, *Senior Member, IEEE*, Stefano Maci, *Fellow, IEEE*

Abstract—The upper limit on the directivity of self-resonant antennas that fit within a minimum sphere is determined for a given quality factor. This formulation is obtained by analytically solving a rigorous convex problem and is expressed as a rapidly converging analytical series. The total quality factor, inverse of the relative frequency bandwidth, is formulated by considering the quality factors of individual spherical waves. From the exact series, approximate closed-form formulas have been derived, which exhibit high accuracy in complementary ranges of the minimum circumscribed sphere's radius. These ranges encompass small antennas as well as intermediate to large antennas. Special emphasis is given to small antennas, where the solution is interpreted as combination of dipolar and quadrupolar Huygens' source contributions with appropriate closed form coefficients. The solution in this range provides continuity to the maximum directivity between 3 and 8 maintaining a constant *Q*.

Index Terms—Super-directivity, antennas, bandwidths, fundamental limits, quality factor, spherical harmonics.

I. INTRODUCTION

Given the recent requirements for highly directive electrically small radiators and scatterers in various communication and sensor applications, there has been a renewed interest in the concept of super-directivity. Super-directivity refers to the ability to achieve exceptionally high levels of directivity, beyond what is traditionally achievable with conventional antenna designs. This renewed interest is driven by the demand for improved performance in terms of range, resolution, and sensitivity in communication and sensing systems.

The definition of the maximum directivity for a given electrical size of the minimum sphere circumscribing the antenna requires a constraint to ensure a finite bound, as without it the directivity could be in principle infinite. This constraint can take the form of a lower limit on the efficiency or an upper limit on the *Q*-factor (i.e., minimum relative frequency bandwidth), among other possibilities. Alternatively, it is also possible to restrict the number of harmonics that can be excited over the minimum sphere based on the degrees of freedom (DoF) of the field. In this paper, our focus is on *Q*-bounded maximum directivity.

The problem of maximum bound of directivity and super-directivity has been studied by many authoritative scientists [1]-[19]. In essence the problem is convex, and therefore our formulation can be aligned within the framework established in [1]. While the formulation in [1] is applicable to general shapes, the one presented here is focused on spherical source regions, with the advantage of resulting in a concise analytical formula. This formula is eventually approximated by a simple and appealing closed form expression, that offers valuable physical insight, particularly for small antennas. The issue of losses

arising from realistic conductivity is not treated here and will be addressed in a companion paper [20].

Assuming sources fitting inside a minimum sphere of radius r_{\min} , the maximum directivity can be found as suggested by Harrington [3]-[5]. His method is based on the expansion of the radiated field in a finite number of spherical waves (SWs), and on the maximization of the directivity with respect to the coefficients of the expansion. This procedure leads to

$$D_{\max} = \sum_{n=1}^{N_{\max}} (2n+1) = \left(N_{\max}\right)^2 + 2N_{\max} \quad (1)$$

where $N_{\max} \geq 1$ is the maximum polar index of the SWs that contribute to the far field for the given minimum sphere. Hence, the maximum directivity depends on the value set for N_{\max} . It was suggested by Harrington that the maximum polar index is the largest integer smaller than kr_{\min} , where k is the free-space wavenumber, i.e., $N_{\max} = \lfloor kr_{\min} \rfloor$ (where $\lfloor \cdot \rfloor$ is the entire part of the argument). This assumption invokes the difficulty to excite SWs with polar index $n > kr_{\min}$ with a sufficiently high intensity over the minimum sphere to significantly contribute to the far field; namely, as underlined in [6], it relies on the finiteness of the number of degrees of freedom (DoF) of the field in the far zone. To put it differently, the Harrington's procedure is grounded in the understanding that the SWs are below cut-off as long as the order of the spherical Hankel function is larger than its argument. This is actually the same concept invoked to establish the number of DoF of the field radiated by sources inside a minimum sphere. We note that according to (1), when $N_{\max} = 1$ the maximum directivity is equal to 3, and it is associated to the Huygens' source.

Since the formula in (1) is discontinuous, Harrington suggested to give it continuity just posing $N_{\max} = kr_{\min}$, thus leading to

$$D_{\max} = \left(kr_{\min}\right)^2 + 2kr_{\min} \quad (2)$$

This extension, while in asymptotic agreement with the DoF concept of truncation, is empirical and manifests its inaccuracy especially in the range kr_{\min} between 1 and 2. In this range, the truncation of the series in (1) leads to only two potential outcomes for maximum directivity, namely 3 (for $N_{\max} = 1$)

and 8 (for $N_{\max} = 2$). The interpolation in equation (2) represents just one possible approach to transition from one to the other with continuity. Other possible formulas have been proposed for small antenna sizes. It was suggested in [6] that the maximum directivity for non-super-reactive antennas can be heuristically defined as $D_{\max} = (kr_{\min})^2 + 2kr_{\min}$ for $kr_{\min} > 1.5$ and $(kr_{\min} + 3)$ for $kr_{\min} < 1.5$; this heuristic extension was compared with some available literature data for very small antennas.

It is well known that there exist antennas, sometimes called “superdirective”, with directivity larger than the limit in (2) even if with small bandwidth. The possibility to exceed the limit in (2) derives from the fact that its derivation does not consider the possibility to excite, with sufficiently large intensity over the minimum sphere, SWs with polar index larger than kr_{\min} . As a matter of fact, increasing the number of super-reactive harmonics over the minimum sphere leads to a diverging Q factor, which is eventually useless for practical antenna applications, since the bandwidth goes to zero. Vice versa, allowing for a certain desired maximum Q may imply a bound of directivity larger than the one derived in (2). The main objective of this paper is therefore to obtain the maximum directivity for a given bandwidth and minimum sphere, and a closed form approximation for it.

In [18], Yaghjian presented simplified formulas for sampling the minimum sphere. He distinguished non-resonant antennas from resonant antennas and provided a link between the equivalent radius associated with the storage of reactive energy and the maximum equivalent area of the antenna, therefore establishing a link with the maximum directivity. Fante [17] proposed a maximization of the product directivity-bandwidth (note that although the title in [17] mentions “gain”, the treatment there is relevant to directivity). The coefficients of the SWs found by Fante are different from the ones found by Harrington and the series is not truncated like in (1). However, the D/Q bound obtained this way is always relevant to small Q (large bandwidth) and moderate D , which is of practical interest only for ultrawideband antennas. In [13], the minimum Q -factor for a given directivity of a small antenna of arbitrary shape is obtained by setting a convex problem and solving it by a semidefinite relaxation technique. In this paper, instead, Q is fixed a priori, and the directivity is maximized.

The paper is structured as follows. Section II derives the limit for Q -bounded maximum directivity. Section III focuses on small resonant antennas, where the maximum directivity is obtained by the combination of dipolar and quadrupolar resonant sources. The Chu limit of bandwidth is extended to the presence of quadrupoles and a closed form formula for small antennas is provided, which allows to have a continuous description of maximum directivity from 3 to 8 for constant Q and for any antenna size. Section IV presents a closed form approximation of the maximum directivity for intermediate to moderately large antennas. Section V shows the maximum directivity in terms of an equivalent radius that contains all the reactive energy. Finally, Section VI gathers the conclusions.

II. Q-BOUNDED MAXIMUM DIRECTIVITY

Let us first refer to the problem in Fig. 1, where the equivalence theorem is applied to the *minimum spherical surface* including all the sources. The Love formulation of the equivalence principle relates the equivalent electric (\mathbf{J}) and magnetic (\mathbf{M}) currents to arbitrary magnetic (\mathbf{H}) and electric (\mathbf{E}) Maxwellian’s fields, though $\mathbf{J} = \hat{r} \times \mathbf{H}$, $\mathbf{M} = \mathbf{E} \times \hat{r}$, where \hat{r} is the normal to the surface. In the Love’s formulation, the field inside the minimum sphere is assumed equal to zero, therefore not equivalent in terms of stored energy to the initial problem. However, since the energy of the equivalent problem is zero inside the sphere, any other source generating the same external fields will lead to a higher Q . The bounds we will find here is therefore more optimistic than the one obtained by electric currents only over a sphere [2], in which the energy can be stored even inside the sphere.

In the rest of the paper we the currents will be expanded in terms of spherical wave harmonics, with coefficients C_i , adopting the normalization of the Hansen’s book [21], for which the radiated power is given by $P_r = \frac{1}{2} \sum_i \hat{a}_i |C_i|^2$

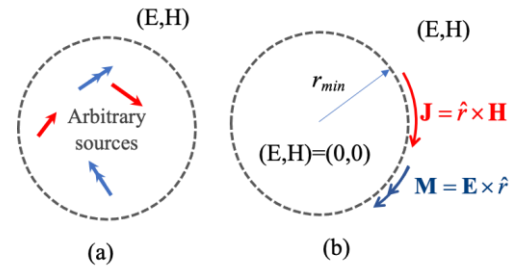


Fig. 1 Application of the equivalence principle to the minimum sphere surface: (a) original problem; (b) equivalent electric and magnetic surface currents radiating in free space with zero field inside (Love formulation).

A. Total Q -factor

The Q -factor can be defined in two different ways depending on whether one assumes to have a self-resonant antenna or an antenna that is made resonant by providing an external reactive energy from a lossless tuning circuit. In the first case, one has $W_e = W_m$, $Q = 2\omega W_e / P_r = 2\omega W_m / P_r$ where ω is the angular frequency, P_r is the radiated power and W_e and W_m are the electric and magnetic stored energies, respectively. For non-resonant antennas, one has $Q = 2\omega W_e / P_r$ for capacitive antennas and $Q = 2\omega W_m / P_r$ for inductive antennas. This definition assumes that an external energy has been added to the system to get the resonance. In both cases, the Q -factor can be interpreted as the reciprocal of the fractional bandwidth $BW = 1/Q$ when it is larger than 10 [15].

The calculation of the stored energies $W_{e,m}$ of a general spherical wave expansion is an old and debated topic [3],[16],[22]-[25]. Essentially, the most used approaches are the ones provided by Chu [26], Collin and Rothschild [15] and Fante [22], the latter generalized to the case of arbitrary field internal to the minimum sphere in [23]. It turns out [17] that the

condition of maximum directivity implies that TE and TM spherical modes with the same indices have coefficients of equal amplitude; under this condition, the Q of the antenna reduces to

$$Q = \frac{\hat{a}_n |c_n|^2 Q_n}{\hat{a}_n |c_n|^2} \quad (3)$$

where Q_n are defined in Appendix A and C_n are the field expansion coefficients for the maximum directivity. The adoption of (3) inherently assumes self-balancing of reactive energy. Consequently, the limit we obtain in the subsequent analysis is relevant to self-resonant antennas, namely antennas characterized by achieving resonance without requiring the provision of energy through an external circuit.

For the sake of convenience, the Fante's Q_n are plotted in Fig. 2 as a function of kr_{\min} for some values of n . The asymptotic behaviour for small and large values of kr_{\min} is given by [23]

$$Q_n \begin{cases} \frac{n \left(\frac{(2n)!}{n! 2^n} \right)^2}{2} \frac{1}{(kr_{\min})^{2n+1}} & \text{for } kr_{\min} \rightarrow 0 \\ a_n (kr_{\min})^{-1} & \text{for } kr_{\min} \rightarrow \infty \end{cases} \quad (4)$$

with $a_n = (a_{n-1} + n)$ and $a_0 \doteq 1$ by definition. It is seen that Q_n exhibits a drastic change of slope for kr_{\min} around n . It is important to note the Fante's Q_n for $n=1$ gives exactly $Q_1 \propto \frac{1}{2}(kr_{\min})^{-3} + (kr_{\min})^{-1}$, which will be shown later to be related to the Chu limit of bandwidth.

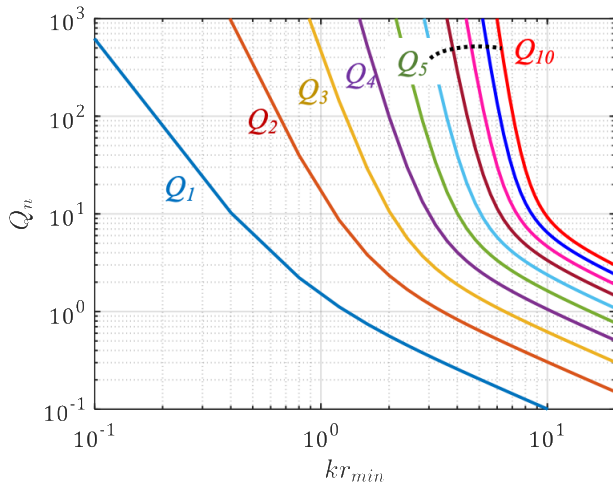


Fig. 2 Fante's Q_n coefficients. The used log-log scale emphasizes the different behavior of Q_n with corner point at $kr_{\min} \gg n$.

B. Analytical form for Q-bounded maximum directivity

The maximum directivity for a given quality factor Q is formulated in terms of the minimization of a convex function. The optimization problem consists on finding the SW

coefficients that maximizes U/P_r where $P_r = \frac{1}{2} \hat{a}_i |C_i|^2$ and $U = \frac{1}{4\rho} |\hat{a}_i C_i K_i|^2$ with

$$K_i = \sqrt{2n+1} \times \begin{cases} 0 & \text{if } |m| = 1 \\ -(-j)^n & \text{TE, } m = \pm 1 \\ -m(-j)^n & \text{TM, } m = \pm 1 \end{cases} \quad (5)$$

where the ‘‘polar’’ index n refers to the order of the Hankel function and the index m refers to the azimuthal angular wave number of the spherical wave expansion. The index $i = 2[n(n+1) + m - 1] + s$ collects the three indexes n, m, s where s assumes values 1 and 2 for transverse electric (TE) and transverse magnetic (TM) polarization, respectively. We note that (5) is congruent with the normalization of the Hansen's book [21], for which the power radiated by an individual harmonic is $\frac{1}{2} |C_i|^2$. The maximization of U/P_r bounded by a certain value of Q is given by

$$\max_{C_i} \frac{|\hat{a}_i C_i K_i|^2}{\hat{a}_i |C_i|^2}; \frac{\hat{a}_n Q_n |c_n|^2}{\hat{a}_n |c_n|^2} \leq Q \quad (6)$$

where Q_n are the Fante's quality factors (Appendix A), and Q is the maximum accepted Q -factor (minimum relative bandwidth). It is important to observe that the inequality in (6) is actually equivalent to an equality, since it comes out that any increase of the amplitude of the higher order coefficients that provides larger directivity also implies an increase of Q . Therefore, finding the maximum directivity for a given maximum Q means in practice finding it for a constant Q .

Since the constraint depends only on the amplitude of the coefficients, the maximum in (6) is achieved by $\nabla C_i = -\nabla K_i$, and therefore by $C_i K_i = |C_i| |K_i| = |C_n| \sqrt{2n+1}$. From now on, we can therefore use the polar index n only, since the amplitude of K_i does not depend on the indexes m and on the polarization. Setting the radiated power so that $\hat{a}_n |C_n|^2 = 1$, the problem in (6) is equivalent to

$$\max_{|C_n|} \left(\sum_n |C_n| \sqrt{2n+1} \right)^2 \text{ with } \sum_n |C_n|^2 = 1; \sum_n Q_n |C_n|^2 = Q \quad (7)$$

We can now reformulate (7) by using its dual problem obtained by combining the constraints with a scalar parameter χ ; i.e.,

$$\min_{\chi} \max_{C_n} \left(\sum_n |C_n| \sqrt{2n+1} \right)^2 \quad (8)$$

subject to $\sum_n [\chi(Q_n - Q) + 1] |C_n|^2 = 1$

The solution of this problem for $Q > Q_1$ is given in Appendix B by the Lagrange multiplier method. The result is

$$D_{\max}(Q, kr_{\min}) = \min_{\chi \in [0, \chi_{\max}]} \sum_{n=1}^{\infty} \frac{2n+1}{\chi(Q_n - Q) + 1} \quad (9)$$

where $\chi_{\max} = 1/(Q - Q_1)$. Eq. (9) explicitly relates the maximum directivity to the bandwidth for any given antenna size. The value $\bar{\chi} = \bar{\chi}(Q, kr_{\min})$ that minimizes the series in (9) is represented in Fig.3 as a function of the kr_{\min} for some fixed values of Q . An excellent approximation of $\bar{\chi}$, valid for $Q_1 \notin Q \notin Q_2$, is given by

$$\bar{\chi} = \frac{8}{3(Q_2 - Q)} \left(-1 + \sqrt{1 - \frac{60(Q_2 - Q)}{256(Q_1 - Q)}} \right) \quad (10)$$

We note that $\bar{\chi}$ tends to diverge when $Q = Q_1$. It can be easily seen, however, that $\bar{\chi}(Q_1 - Q)$ in the denominator of (9) goes to zero, while all the other terms of the series are negligible, due to the high values of $\bar{\chi}(Q_n - Q)$ for $n \neq 1$. Therefore D_{\max} tends to 3 for any Q that tends to Q_1 . This is expected since in the quasi static limit a sphere can contain only one self-resonant source, which is the Huygen's dipole.

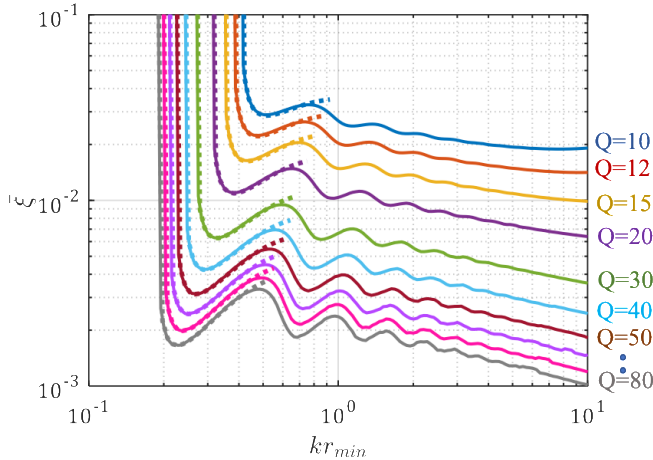


Fig. 3. Parameter $\bar{\chi}$ that minimizes the summation in (9) (continuous line) and its approximation in (10) (dashed line) truncated at $Q = Q_2$, for various values of Q ($Q=10,12,15,20,30,40,50,60,70,80$).

The envelope of the terms inside the summation in (9) are plotted in Fig. 4. For low values of Q , the coefficients envelope reaches a maximum close to $n = kr_{\min}$, while for large Q the maximum moves toward higher values, being defined by $Q = Q_n$. Let us define the quantity kr_n , as follows:

$$kr_n \text{ such as } Q = Q_n \quad (11)$$

For $n > r_n$, the coefficients exhibit a fast decay, with a rate that depends on kr_{\min} and Q . This behavior is due to the change of the decay rate of Q_n when crossing kr_n (see Fig. 2). An approximation of kr_n for values of Q larger than 100, $kr_{\min} < 2$ and $n < 12$ is

$$kr_n \gg \frac{n}{1.356Q^{1/(2n+1)}} \quad (12)$$

The above formula is useful for the approximation that will be presented in the Sec. IV.

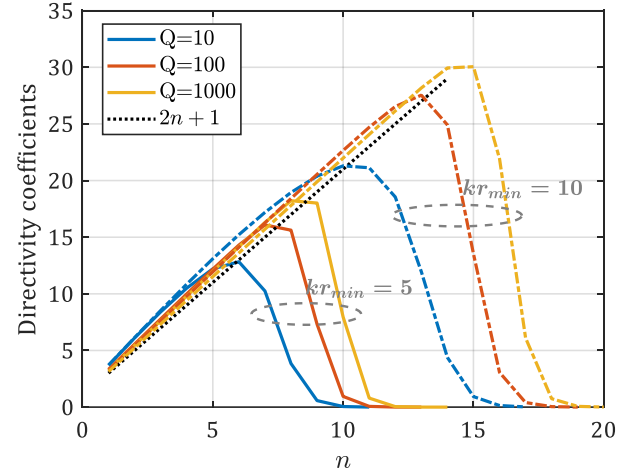


Fig. 4 Envelope of the maximum directivity summation terms in (9) for three values of Q , namely $Q = 10, Q = 100$, and $Q = 1000$, for two values of kr_{\min} . The dotted black line represents the envelope of the corresponding Harrington coefficients for maximum directivity.

C. SW coefficients for maximum directivity

The maximum directivity for constant Q is obtained with field coefficients

$$C_{i,\max}^{(Q)} = \frac{C_0 \sqrt{2n+1}}{\bar{\chi}(Q_n - Q) + 1} \times \begin{cases} 0 & \text{if } |m| \neq 1 \\ -(j)^n & \text{TE, } m = \pm 1 \\ -m(j)^n & \text{TM, } m = \pm 1 \end{cases} \quad (13)$$

where C_0 is an arbitrary constant. Note that for $\bar{\chi}(Q_n - Q) \ll 1$ the coefficients $C_{i,\max}^{(Q)}$ recover the coefficients obtained by Harrington for the case of finite number of SWs without imposing the Q -bound, and just invoking the truncation of the series. It should be stressed that the set of SW coefficients in (13) implies that electric and magnetic energy are equal each other for $r > r_{\min}$ for any polar index; namely, the maximization is relevant to self-resonant antennas. The envelope of the amplitude of the coefficients in (13) in dB scale is given in Fig. 5 for two values of Q ($Q = 10$ and $Q = 100$) and various values of kr_{\min} ; the arbitrary constant C_0 is set to unity in the calculations.

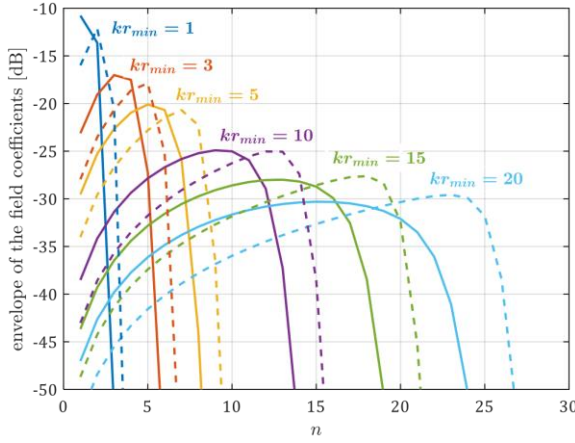


Fig. 5 Envelope of the amplitude of the coefficients in (13) for various values of kr_{\min} and two values of Q , namely $Q = 10$ (continuous line) and $Q = 100$ (dashed line). The arbitrary constant C_0 has been set to unity.

D. D_{\max} vs kr_{\min} for constant Q

Fig. 6 shows the maximum directivity D_{\max} in a range of $kr_{\min} \hat{1} (0.1;10)$ for various values of Q . The directivity value is truncated at 3, which corresponds to the condition $Q = Q_1$. This situation is associated to the Chu limit, as will be discussed next. For the sake of comparison, the Harrington formula in (2) is also included, represented by black dash-dotted line. We should however consider that the latter does not provide the same Q for any value of the minimum radius. The dotted lines correspond to a closed-form approximation provided in Sec. III-D and IV in their respective fields of validity.

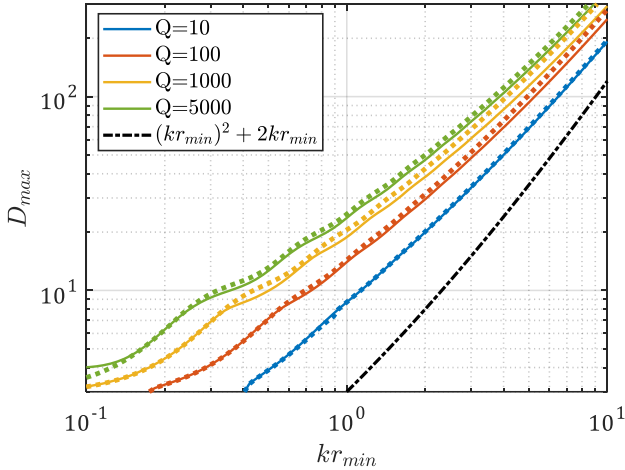


Fig. 6 Maximum directivity (log-log scale) for constant Q . The curves are truncated at the corresponding Chu limit radius, where $D_{\max}(Q, kr_{\min}) \gg 3$. Comparisons of the exact formula (9) (continuous line) and the combination between (23) and (28) (dotted line-lines) for $Q = 10, Q = 100, 1000, 5000$.

III. SMALL ANTENNAS: DIPOLAR AND QUADRUPOLAR RESONANT SOURCES

From the previous analysis it can be seen that the n -th spherical harmonics, either TE and TM with azimuthal index $m = \pm 1$ have the same Q_n and the same coefficients' amplitude

for providing maximum directivity. This is true for both the Harrington's coefficients (conjugate of (5)) and the Q -bounded ones derived in (13). For $n = 1$, the resulting radiated field can be interpreted as the one produced outside the minimum sphere by an elementary Huygens' dipole (HD) located at the origin (Fig. 7a). The latter is constituted by a couple of horizontal electric and magnetic dipoles with momenta related by the free space impedance Z (i.e., $ID\ell = MD\ell/Z$). By duality, the energy density of the HD is balanced outside the minimum sphere aligning with the self-resonant formulation we have adopted. Huygens' source antennas have been successfully implemented in practical applications, ranging from electrically small packages [27]-[29] to larger ones [30]-[31]. Their significance as a research area has been acknowledged, particularly for Internet of Things (IoT) applications [32]. Furthermore, Huygens' metasurfaces have already demonstrated their effectiveness in antenna and scattering problems [32]- [36].

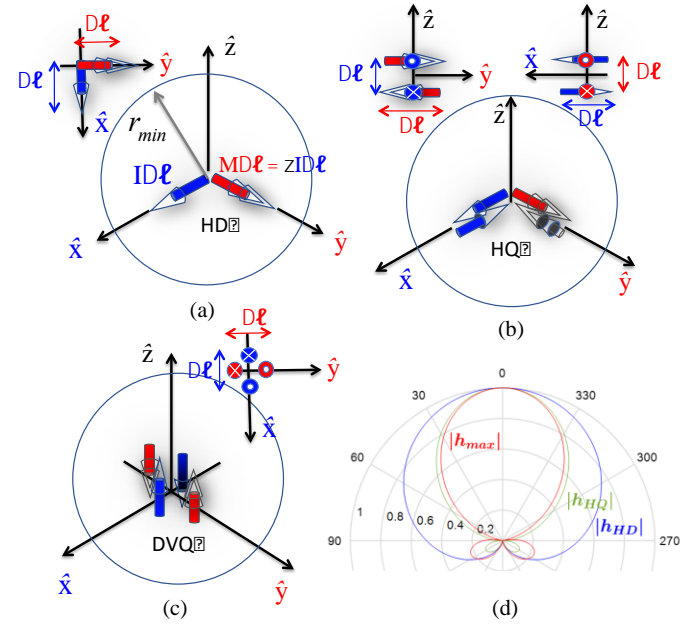


Fig. 7 Graphical representation of a (a) Huygens' dipole (HD), (b) Huygens' Quadrupole (HQ) and (c) Dual Vertical Quadrupole (DVQ) (d) normalized radiation patterns of HD, HQ and combination of HD, HQ and DVQ for maximum directivity.

The combination of the spherical wave harmonics for $n = 2$ provides the field of a Huygens' Quadrupole (HQ) combined with the one of a Dual Vertical Quadrupole (DVQ). Graphical representations of the HQ and DVQ are given in Fig. 7b and 7c, respectively. The HQ is composed by pairs of counterdirected HDs separated by a vanishingly small electrical distance. The HQs have been recently studied in the problem on needle radiation from an array [37]. The DVQ is a combination of closely counterdirected vertical magnetic and electric dipoles, where the displacement of the electric dipoles is along x and the one of the magnetic dipoles is along y . Like the HD, the HQ and DVQ provide balanced energy outside the minimum sphere, due to duality. The normalized far-field radiation pattern expression of HD, HQ and DVQ are given by

$$\mathbf{h}_{\text{HD}} = \frac{1}{2}(\cos q + 1)\hat{\mathbf{p}} \quad (14)$$

$$\mathbf{h}_{\text{HQ}} = \frac{1}{2}(\cos q + 1)\cos q\hat{\mathbf{p}} \quad (15)$$

$$\mathbf{h}_{\text{DVQ}} = \sin^2 q\hat{\mathbf{p}} \quad (16)$$

$$\hat{\mathbf{p}} = [\cos f\hat{\mathbf{q}} - \sin f\hat{\mathbf{f}}] \quad (17)$$

where $\hat{\mathbf{p}}$ is a unit polarization vector. The individual directivity of isolated \mathbf{h}_{HD} , and \mathbf{h}_{HQ} are 3 and 7.5, respectively. We note that the condition of maximum directivity for $n = 2$ links the coefficients of HQ and DVQ each other combining it as follows

$$\mathbf{h}'_{\text{HQ}} = \mathbf{h}_{\text{HQ}} - \frac{1}{2}\mathbf{h}_{\text{DVQ}} = \frac{1}{2}(\cos q + \cos 2q)\hat{\mathbf{p}} \quad (18)$$

The normalized far-field radiation pattern of \mathbf{h}_{HD} , \mathbf{h}_{HQ} and \mathbf{h}'_{HQ} are shown Fig. 7d. We note that the *exact* form of Q_1 and Q_2 are given by

$$Q_1 \circ \frac{1}{2(kr_{\min})^3} + \frac{1}{(kr_{\min})} \quad (19)$$

$$Q_2 \circ \frac{9}{(kr_{\min})^5} + \frac{9}{2(kr_{\min})^3} + \frac{3}{kr_{\min}} \quad (20)$$

These two expressions can be interpreted as the quality factors of *isolated* HD and HQ, respectively.

A. Minimum Q for Isolated Huygens' dipole (Chu limit)

Before proceeding further, we should note that the condition $Q \geq Q_1$ provides a lower bound for the Q -factor (upper bound for the maximum bandwidth) for small antennas; this can be identified as the well know Chu limit. We note, however, that in [26] Chu defined the limit for omni-directional antennas by considering only the TM modes, thus providing $Q \geq Q_{\text{Chu}}^{(\text{TM})} = 1/(kr_{\min})^3 + 1/(kr_{\min})$. In [38], McLean emphasizes that the limit changes when considering both TE and TM modes, with special emphasis to the circular polarization. The latter corresponds to two vertical electric and magnetic dipoles with balanced energy. In this case, the dominant quasi-static term is weighted by a factor 2 at the denominator; that identifies $Q \geq Q_1$ as the Chu limit. Indeed, in [26] and [38] the authors did not consider the case of maximum directivity, but the case of antennas isotropic in the azimuthal plane. In case of maximum directivity and self-resonant antennas, the present formulation naturally recovers an HD instead of two vertical dipoles since the HD gives the maximum directivity. With the above clarification we will refer anyway to the condition $Q \geq Q_1$ as the Chu limit.

B. Minimum Q for isolated Huygens' Quadrupole

It is seen from (20) that the generalization of the Chu limit to isolated HQ leads to $Q \geq Q_2$. This is much more restrictive in terms of bandwidth than $Q \geq Q_1$; that is, it provides a relative bandwidth $0.11(kr_{\min})^5$ in the dominant low frequency term; however, HQ gives a higher directivity with respect to HD (7.5

vs 3). The maximum possible directivity is however obtained by a proper combination of dipolar and quadrupolar contributions, as shown below.

C. Combination of dipolar and quadrupolar contributions for maximum directivity.

Let us combine the dipolar and quadrupolar contributions \mathbf{h}_{HD} and \mathbf{h}'_{HQ} with arbitrary coefficients, namely $\mathbf{h} = \mathbf{h}_{\text{HD}} + g \mathbf{h}'_{\text{HQ}}$ where g is a real number. The directivity can be calculated as $D = 2/\int_0^\pi |\mathbf{h}|^2 / |\mathbf{h}|_{\text{max}}^2 \sin q dq$, leading to

$$D = 3 \frac{(1+g)^2}{1+\frac{3}{5}g^2} \quad (21)$$

This directivity exhibits a maximum at $D_{\text{max}} = 8$ for $g = 5/3$. This result is in agreement with the results obtained by the Harrington's coefficients, and leads to a total Q equal to

$$Q^{(2)} = \frac{3Q_1 + 5Q_2}{8} = \frac{45}{8(kr_{\min})^5} + \frac{3}{(kr_{\min})^3} + \frac{2}{(kr_{\min})} \quad (22)$$

The latter is the quality factor that can be obtained with dipolar and quadrupolar contributions combined for maximum directivity. This result implies a relative bandwidth of $0.17(kr_{\min})^5$ at low frequency, which is larger than that of the HQ alone. In Fig. 8, the points described by $Q = Q_1$, $D_{\text{max}} = 3$ and $Q = Q^{(2)}$, $D_{\text{max}} = 8$ are set in a diagram D_{max} Vs Q for several values of kr_{\min} . The dots are connected with straight dashed lines. For comparison, our solution in (9) is plotted in the same figure. The latter covers with continuity the range from max directivity 3 to 8 with minimum Q (continuous line).

D. Combination of dipolar and quadrupolar contributions with Q bound.

Imposing a bound to Q and truncating the series in (9) at the first two terms leads to the combination $\mathbf{h} = \mathbf{h}_{\text{HD}} + g \mathbf{h}'_{\text{HQ}}$, resulting in $Q = (Q_1 + \frac{3}{5}\gamma^2 Q_2) / (1 + \frac{3}{5}\gamma^2)$; deriving γ from the latter leads to $g = \sqrt{5(Q - Q_1) / (3(Q_2 - Q))}$ which substituted in (21) yields

$$D_{\text{max}} = 3 \frac{(\sqrt{Q_2 - Q} + \sqrt{\frac{5}{3}(Q - Q_1)})^2}{Q_2 - Q_1}; \quad Q_1 \leq Q \leq Q^{(2)} \quad (23)$$

Note that, even if the above equation exists for $Q_1 \leq Q \leq Q^{(2)}$, the result is representative of the maximum achievable directivity for Q bound only in the range $Q_1 \leq Q \leq Q^{(2)}$. In $Q^{(2)}$ the directivity assumes the maximum value equal to 8, touching the Harrington point and then decreases (see Fig. 8). Note that the same result can be obtained by truncating the series in (9), setting to zero the derivative and solving the resulting second

order equation with the proper branch in \mathcal{X} . It results therefore that the combination of dipolar and quadrupolar contributions that leads to the minimum Q and maximum directivity for any antenna size is

$$\mathbf{h} \gg \mathbf{h}_{HD} + \sqrt{\frac{5(Q - Q_1)}{3(Q_2 - Q)}} \mathbf{h}'_{HQ} \quad Q_1 \leq Q \leq Q^{(2)} \quad (24)$$

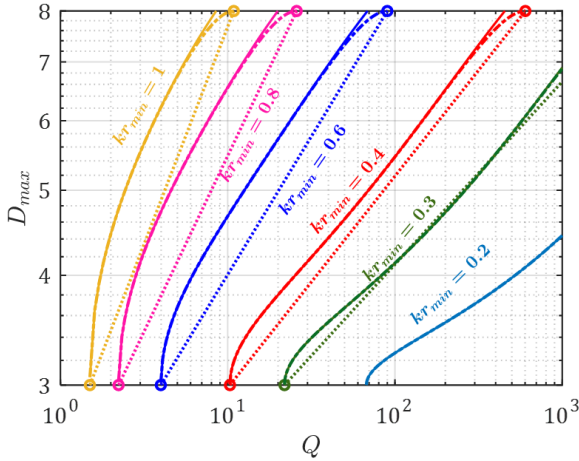


Fig. 8 Maximum directivity as a function of the Q . Dots (connected by dashed lines) are obtained by $Q = Q^{(2)}$ ($D_{\max} = 8$) and by $Q = Q_1$ ($D_{\max} = 3$). Continuous lines are obtained through (9). Dash-dotted lines are obtained by using (23), namely setting Q constant for dipolar and quadrupolar contributions. The solution minimally deviates around $Q = Q^{(2)}$ with respect to eq. (9) since the latter includes the contribution of order 3 (hexapoles).

The accuracy of (23) when compared with the exact solution is good in the range of maximum directivity $3 \leq D_{\max} \leq 8$ (dash-dotted line in Fig. 8, in comparison with the exact solution). We stress that this range of directivity corresponds to $Q_1 \leq Q \leq Q_2$, or in terms of antenna size

$$kr_1 \leq kr_{\min} \leq kr^{(2)} \gg 0.9kr_2 \quad (25)$$

where kr_1, kr_2 , and $kr^{(2)}$ are the values for which $Q = Q_1, Q = Q_2$, and $Q = Q^{(2)}$, respectively. The values of $kr_1, kr^{(2)}$, and kr_2 a function of Q are obtained by inverting (19), (20), and (22) and can be approximated as

$$kr_1 \approx 0.4 \left(\frac{1}{Q} + \frac{2}{Q^{1/3}} \right) \quad (26)$$

$$kr^{(2)} \approx 1.42 \left(\frac{1}{Q} + \frac{1}{Q^{1/5}} \right) = 0.9kr_2 \quad (27)$$

Comparison of the exact form (9) (continuous line) with the two terms approximation in (23) (dashed lines) is shown in Fig. 9 for several values of Q . The percentage relative error of Eq. (23) with respect to the full expansion in the range

$kr_1 \leq kr_{\min} \leq 0.8kr_2$ is less than 1% for $100 \leq Q \leq 1000$ and less than 4% for $10 \leq Q \leq 100$, with maximum error always obtained close to $0.8kr_2$.

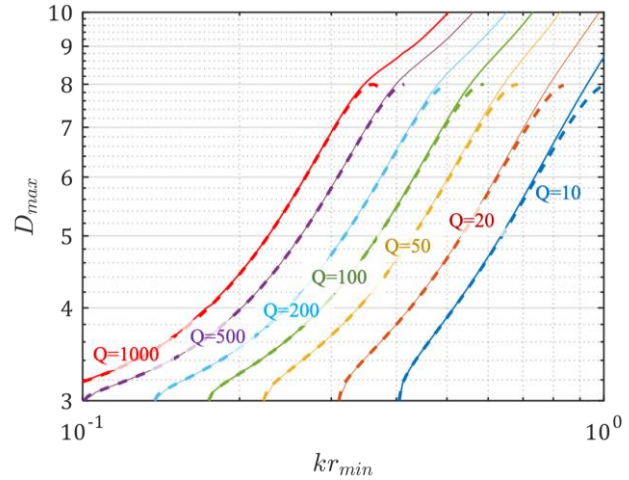


Fig. 9 Bound of frequency bandwidth constrained maximum directivity (log-log scale) for different values of Q , truncated at the corresponding Chu limit radius, where $D_{\max}(Q, kr_{\min}) = 3$. Comparison between the exact formula (9) (continuous line) and the approximate formula for small antennas in (23) (dashed lines). The dashed curves are plotted for $kr_1 \leq kr_{\min} \leq 0.8kr_2$.

E. Multipole contributions without and with Q bounds.

For completeness, Fig. 10 shows D_{\max} as a function of Q for various values of kr_{\min} associated to a finite number N_{\max} of multipoles order. To this end, the expression $D_{\max} = (N_{\max})^2 + 2N_{\max}$ is evaluated as a function of $Q = \hat{a}_{n=1}^{N_{\max}} Q_n (2n+1) / (N_{\max}^2 + 2N_{\max})$. The latter expression corresponds to the finite number of harmonics weighed by the Harrington coefficients (the latter given by the conjugate of (5)). The Fante's Q_n have been used in the calculations. This plots can be obtained only by discrete points since N_{\max} can assume only integer values. These points are connected by straight lines in Fig. 10. The continuous curve is obtained by the exact formula (9). It is seen that the discrete points are reasonably close to the continuous curve obtained by (9), and always below the continuous curve.

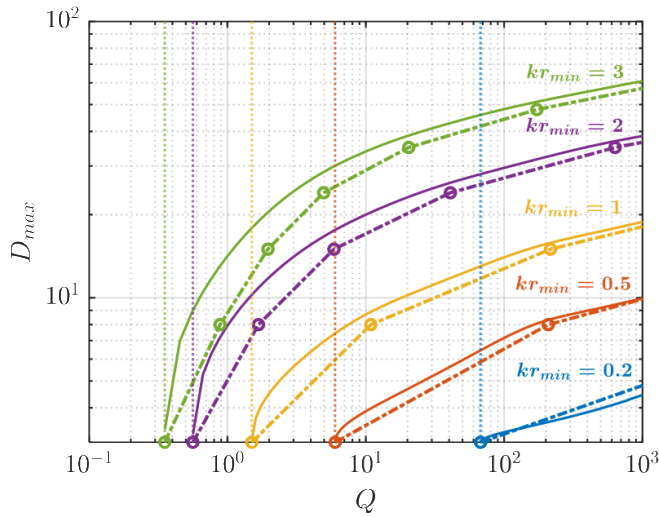


Fig. 10 Maximum directivity as a function of Q from the Harrington's coefficients (dots, connected by dashed lines) derived from (9) (dashed lines) for different values of kr_{\min} from 0.2 to 3. The vertical dotted lines correspond to the Chu-limit $Q = Q_1$.

IV. CLOSED-FORM FORMULAS FOR $0.6kr_2 < kr_{\min} < 10$

It is seen from Fig. 3 that the value of $\bar{\chi}$ is smoothly varying for $kr_{\min} \notin kr_2$. Just adopting the value that $\bar{\chi}$ possesses in $0.6kr_2$ and maintaining it all-over the range $0.6kr_2 < kr_{\min} < 10$ provides a quite accurate solution for the directivity. This value, derived directly from (10), leads to $\bar{\chi} \gg 0.285/Q$, thus, providing the compact closed form

$$D_{\max}^{(approx)} \approx \sum_{n=1}^{\infty} \frac{(2n+1)}{0.16 \left(\frac{Q_n}{Q} - 1 \right) + 1} \quad (28)$$

We observe that the summation can be truncated at $\lceil kr_{\min} \rceil + 10$ without compromising the accuracy. Comparison between the exact form in (9) and the one in (28) is given in Fig. 6. It is seen that this formula is accurate for $0.8kr_2 \notin kr_{\min} \notin 20$ and $10 < Q < 5000$. In particular, the percentage error $e\% = (D_{\max}^{(approx)} - D_{\max}) / D_{\max}$ in the above range for various values of Q is presented in Fig. 11. It can be seen that the percentage error is less than 5% for $Q < 100$ and less than 7% for $Q < 1000$.

V. EQUIVALENT RADIUS CONTAINING THE REACTIVE ENERGY

We can evaluate the ratio between the equivalent radius obtained by $D_{\max} = (kr_{eq})^2$ and the radius of the minimum sphere; r_{eq} may be interpreted as the equivalent radius at which the reactive field becomes negligible [18]. Fig. 12 compares the results for different values of Q with the ones obtained from the directivity estimated by Harrington.

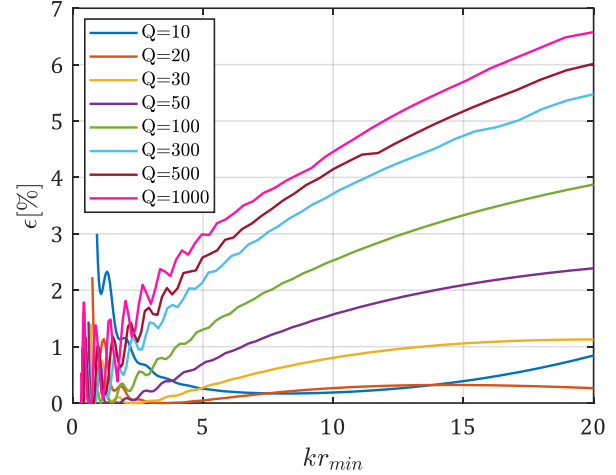


Fig. 11 Percentage error between Bound of maximum directivity between the exact formula (9) for $Q = 10, 100, 1000$ in the range of antenna size $0.8kr_2 \notin kr_{\min} \notin 20$.

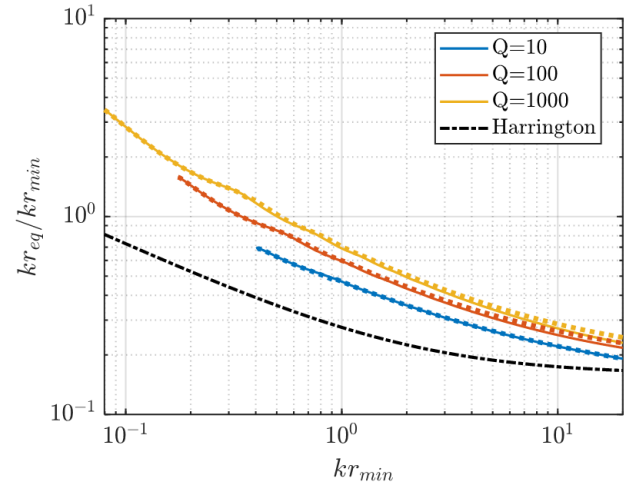


Fig. 12 Ratio between r_{eq} and r_{\min} as a function of kr_{\min} for different values of Q , (the curves are truncated at radius corresponding to the Chu limit). The equivalent radius is obtained from the exact formula (9) (continuous lines) and the approximated ones in (28) (colored dotted lines). The black dashed line is obtained with the Harrington formula in eq. (2) i.e., $(kr_{\min})^2 + 2(kr_{\min})$.

VI. CONCLUSIONS

We have presented an exact analytical expression (eq. (9)) for the maximum antenna directivity with a limit of bandwidth, as a function of the antenna electrical size. The expression has been obtained by solving a convex optimization problem formulated in terms of a spherical wave expansion of the radiated field, and it is expressed in the form of a series that converges rapidly in a large range of the parameters' variation. The main achievements connected with this expression are summarized here.

- i. The coefficients of the SW expansion providing the maximum directivity are given in analytical form, thus,

allowing for the derivation of the optimal radiation pattern for any radius of the minimum sphere.

- ii. The maximum directivity limit goes to 3 for the values of kr_{\min} that respect the Chu limit for dipolar Huygens' dipole. There, the exact formula predicts maximum directivity equal to 3 independently from the value of Q .
- iii. For small antennas, the results are interpreted in terms of a combination of the field radiated by dipolar and quadrupolar Huygens' source outside the minimum sphere. This interpretation leads to the simple formula (23) which provides an accurate continuous description of directivity in the range $3 \leq D_{\max} \leq 8$ as a function of the minimum Q for any fixed antenna size.
- iv. As intermediate step of the solution for small size antennas, we have also found the relation $Q > Q_2$ which established the limit of bandwidth for Huygens' quadrupoles alone, which is an extension of the Chu limit to isolated resonant quadrupoles.
- v. By using the exact formula, a simple analytical closed-form expression has been derived which complements the expression in the quadrupole range for electrical size till $kr_{\min} = 20$ and $Q < 5000$.

We should stress that being the limit obtained with zero field inside the minimum sphere, this limit could be very difficult to approach for large antenna sizes. For small to intermediate size antennas, the simplicity of the final formulas together with its interpretation renders this work useful for antenna engineers. The extension of this work to account for losses will be carried out in a dedicated paper.

ACKNOWLEDGMENTS

This study is financed by Huawei Technologies Co., Ltd., within the joint Innovation Antenna Lab between Huawei and the Department of Information Engineering and Mathematics of the University of Siena. The authors wish to thank Olav Breinbjerg, Rick Ziolkowski, Alejandro Murillo, Zhi Gong and Bruno Biscontinini from for useful and stimulating discussion on this subject. Special thanks to Arthur Yiaghjian for suggesting the introduction of Figs. 8 and 10 (D_{\max} vs Q) and the comparison with the Harrington points.

APPENDIX A: Q-FACTORS FOR SPHERICAL WAVES

The analytical expression of the Fante's Q_n is $Q_n = \frac{1}{2}(Q_n^c + Q_n^d)$, where

$$Q_n^c = x - |h_n(x)|^2 \left[\frac{1}{2}x^3 + x(n+1) \right] - \frac{1}{2}x^3 |h_{n+1}(x)|^2 + \frac{1}{2}x^2 (2n+3) [j_n(x)j_{n+1}(x) + y_n(x)y_{n+1}(x)] \quad (29)$$

$$Q_n^d = x - \frac{1}{2}x^3 \left[|h_n(x)|^2 - j_{n-1}(x)j_{n+1}(x) - y_{n-1}(x)y_{n+1}(x) \right] \quad (30)$$

where $x = kr_{\min}$ and h_n, j_n, y_n and are the spherical Hankel of second kind, Bessel, and Neumann functions of order n , respectively.

APPENDIX B: SOLUTION OF (8)

We can solve the problem in (8) by using the Lagrange multiplier method [39]. To this end, we define the Lagrangian function

$$\mathcal{L}(A_n, I) = \left(\sum_n A_n |K_n| \right)^2 - I \left(\sum_n [x(Q_n - Q) + 1] A_n^2 - 1 \right) \quad (31)$$

where $A_n = |C_n|$ and $|K_n| = \sqrt{2n+1}$. The problem is formulated so that the minimum with respect to ξ of the value λ which maximises the Lagrangian represents the maximum directivity with a certain Q -bound. In order to find this value, (31) is differentiated with respect to I and to A_m and the derivative is set to zero

$$\frac{\partial \mathcal{L}(A_n, I)}{\partial A_m} = 2|K_m| \sum_n A_n |K_n| - 2I [x(Q_m - Q) + 1] A_m = 0 \quad (32)$$

$$\frac{\partial \mathcal{L}(A_n, I)}{\partial I} = \sum_n [x(Q_n - Q) + 1] A_n^2 - 1 = 0 \quad (33)$$

while (33) ensures the respect of the bound in Q after minimization, eq. (32) is satisfied if and only if

$$\frac{\partial}{\partial A_n} A_n |K_n| = I \quad \text{and} \quad |K_m| = [x(Q_m - Q) + 1] A_m \quad (34)$$

Substituting the second equality in the first equality of (34) and using $|K_n| = \sqrt{2n+1}$ leads to

$$I = \sum_n \frac{2n+1}{[x(Q_n - Q) + 1]} \quad (35)$$

from which the maximum directivity is obtained minimizing wrt x . The range of variation of x is determined by imposing that the constraint terms are non-negative, $x(Q_n - Q) + 1 \geq 0 \quad \forall n$; i.e.,

$$Q_n > Q \quad x \geq \max \left\{ -\frac{1}{(Q_n - Q)} \right\} = 0 \quad (36)$$

$$Q_n < Q \quad x \leq \min \left\{ \frac{1}{(Q - Q_n)} \right\} = \frac{1}{(Q - Q_1)}$$

which leads to (9).

REFERENCES

- [1] M. Gustafsson and M. Capek, "Maximum gain, effective area, and directivity," *IEEE Transactions on Antennas and Propagation*, vol. 67, no. 8, pp. 5282–5293, 2019.
- [2] L. Jelinek and M. Capek, "Optimal currents on arbitrarily shaped surfaces," *IEEE Trans. Antennas Propag.*, vol. 65, pp. 329–341, Jan. 2017.
- [3] R. F. Harrington, "Effect of antenna size on gain, bandwidth, and efficiency," *Journal of Research of the National Bureau of Standards-D. Radio Propagation*, vol. 64D, no. 1, Jan.-Feb. 1960.

- [4] R. F. Harrington, "Antenna excitation for maximum gain," *IEEE Trans. Antennas Propag.*, vol. AP-13, no. 6, pp. 896–903, Nov. 1965.
- [5] R. F. Harrington, "On gain and beamwidth of directional antennas," *IRE Trans. Antennas Propag.*, pp. 219–225, July 1958.
- [6] P.-S. Kildal, E. Martini, and S. Maci, "Degrees of freedom and maximum directivity of antennas: A bound on maximum directivity of nonsuper-reactive antennas," *IEEE Antennas and Propagation Magazine*, vol. 59, no. 4, pp. 16–25, 2017.
- [7] A. Yaghjian and S. Best, "Impedance, bandwidth, and Q of antennas," *IEEE Transactions on Antennas and Propagation*, vol. 53, no. 4, pp. 1298–1324, 2005.
- [8] A. D. Yaghjian, T. H. O'Donnell, E. E. Altshuler, and S. R. Best, "Electrically small supergain end-fire arrays," *Radio Sci.*, vol. 43, p. RS3002, 2008. doi: 10.1029/2007RS003747
- [9] E. E. Altshuler, T. H. O'Donnell, A. D. Yaghjian, and S. R. Best, "A monopole superdirective array," *IEEE Trans. Antennas Propag.*, vol. 53, no. 8, pp. 2653–2661, Aug. 2005.
- [10] O. S. Kim, S. Pivnenko, and O. Breinbjerg, "Superdirective magnetic dipole array as a first-order probe for spherical near-field antenna measurements," *IEEE Trans. Antennas Propag.*, vol. 60, no. 10, pp. 4670–4676, Oct. 2012.
- [11] R. C. Hansen, "Fundamental limitations in antennas," *Proc. IEEE*, vol. 69, no. 2, pp. 170–182, Feb. 1981.
- [12] P.-S. Kildal, A. Vosoogh and S. Maci, "Fundamental directivity limitations of dense array antennas: A numerical study using hanna's embedded element efficiency," *IEEE Antennas Wireless Propag. Lett.*, Aug. 2015.
- [13] B. L. G. Jonsson, S. Shi, L. Wang, F. Ferrero, and L. Luzzi, "On methods to determine bounds on the Q-factor for a given directivity," *IEEE Trans. Antennas Propag.*, vol. 65, no. 11, pp. 5686–5696, 2017.
- [14] M. Gustafsson, D. Tayli, and M. Cismasu, *Physical bounds of antennas*. Springer-Verlag, 2015, pp. 1–32.
- [15] R. E. Collin and S. Rothschild, "Evaluation of antenna Q," *IEEE Trans. Antennas Propag.*, vol. 12, no. 1, pp. 23–27, 1964.
- [16] G. A. E. Vandenbosch, "Reactive Energies, Impedance, and Q-Factor of Radiating Structures," *IEEE Transactions on Antennas and Propagation*, vol. 58, no. 4, pp. 1112–1127, April 2010.
- [17] R. Fante, "Maximum possible gain for an antenna with specific Quality Factor" *IEEE Trans on Antennas and Propagat*, vol. 40, no. 12, Dec 1992.
- [18] A. D. Yaghjian, "Sampling criteria for resonant antennas and scatterers," *J. Appl. Physics*, vol. 79, no. 10, pp. 7474–7482, 1996.
- [19] A. Clemente, M. Pigeon, L. Rudant and C. Delaveaud, "Design of a Super Directive Four-Element Compact Antenna Array Using Spherical Wave Expansion," in *IEEE Transactions on Antennas and Propagation*, vol. 63, no. 11, pp. 4715–4722, Nov. 2015.
- [20] L. Passalacqua *et al.* "Maximum Limit of Antenna Gain Without and With Q-bound" Submitted for publication in *IEEE Transactions on Antennas and Propagation*
- [21] J.E. Hansen, & Institution of Electrical Engineers, *Spherical near-field antenna measurements*. London, U.K.: P. Peregrinus on behalf of the Institution of Electrical Engineers, 1988.
- [22] R. Fante, "Quality factor of general ideal antennas," *IEEE Transactions on Antennas and Propagation*, vol. 17, no. 2, pp. 151–155, 1969.
- [23] T. V. Hansen, O. S. Kim and O. Breinbjerg, "Stored Energy and Quality Factor of Spherical Wave Functions—in Relation to Spherical Antennas with Material Cores," *IEEE Transactions on Antennas and Propagation*, vol. 60, no. 3, pp. 1281–1290, March 2012.
- [24] M. Capek, V. Losenicky, L. Jelinek, and M. Gustafsson, "Validating the characteristic modes solvers," *IEEE Transactions on Antennas and Propagation*, vol. 65, no. 8, pp. 4134–4145, 2017.
- [25] R. Harrington, *Time-Harmonic Electromagnetic Fields*. ser. IEEE Press Series on Electromagnetic Wave Theory. Wiley, 2001. Available online at: <https://books.google.it/books?id=4-6kNAEACAAJ>.
- [26] L. J. Chu, "Physical limitations of omni-directional antennas," *Journal of Applied Physics*, vol. 19, no. 12, pp. 1163–1175, Dec 1948.
- [27] P. Jin and R. W. Ziolkowski, "Metamaterial-Inspired, Electrically Small Huygens Sources," *IEEE Antennas Wireless Propag. Lett.* 9, 501 (2010).
- [28] M.-C. Tang, H. Wang, and R. W. Ziolkowski, "Design and Testing of Simple, Electrically Small, Low-Profile, Huygens Source Antennas with Broadside Radiation Performance," *IEEE Trans. Antennas Propag.* 64, 4607 (2016).
- [29] M.-C. Tang, T. Shi, and R.W. Ziolkowski, "Electrically Small, Broadside Radiating Huygens Source Antenna Augmented with Internal Non-Foster Elements to Increase Its Bandwidth," *IEEE Antennas Wireless Propag. Lett.* 16, 712 (2016).
- [30] B. Q. Wu and K.-M. Luk, "A Broadband Dual-Polarized Magneto-Electric Dipole Antenna with Simple Feeds," *IEEE Antennas Wireless Propag. Lett.* 8, 60 (2008).
- [31] K.-M. Luk and B. Wu, "The Magnetolectric Dipole—A Wideband Antenna for Base Stations in Mobile Communications," *Proc. IEEE* 100, 2297 (2012).
- [32] M. Pigeon, C. Delaveaud, L. Rudant, and K. Belmakkadem, "Miniature Directive Antennas," *Int. J. Microw. Wireless Tech.* 6, 45 (2014).
- [33] A. Epstein and G.V. Eleftheriades, "Passive Lossless Huygens Metasurfaces for Conversion of Arbitrary Source Field to Directive Radiation," *IEEE Trans. Antennas Propag.* 62, 5680 (2014).
- [34] J. P. S. Wong, M. Selvanayagam, and G. V. Eleftheriades, "Design of Unit Cells and Demonstration of Methods for Synthesizing Huygens Metasurfaces," *Photonic Nanostruct.* 12, 360 (2014).
- [35] A. Epstein, J. P. S. Wong, and G. V. Eleftheriades, "Cavity-Excited Huygens' Metasurface Antennas for Near-Unity Aperture Illumination Efficiency from Arbitrarily Large Apertures," *Nat. Commun.* 7, 10360 (2016).
- [36] R. W. Ziolkowski, "Low Profile, Broadside Radiating, Electrically Small Huygens Source Antennas," *IEEE Access* 3, 2644 (2015).
- [37] R. W. Ziolkowski, "Using Huygens Multipole Arrays to Realize Unidirectional Needle-Like Radiation" *Physical Review X*, 7, 031017, 2017
- [38] J. S. McLean, "A re-examination of the fundamental limits on the radiation Q of electrically small antennas," in *IEEE Transactions on Antennas and Propagation*, vol. 44, no. 5, pp. 672–676, May 1996, doi: 10.1109/8.496253.
- [39] Boyd S, Vandenberghe L. *Convex optimization*. Cambridge university press; 2004.



Laura Passalacqua (S'21) received her B.Sc. in Informatics and Information Engineering in 2018, followed by an M.Sc. in Electronics and Communications Engineering in 2020, both from University of Siena, Siena, Italy. Since November 2020, she is a PhD student at the University of Siena, Siena, Italy. Her current research of interests include the Degrees of Freedom of electromagnetic fields, analytical and numerical methods for antenna characterization, super-directive and super-gain antenna.



Cristina Yepes (M'19) received the M.Sc. degree in telecommunication engineering from the University of Navarra, Navarra, Spain, in 2015 and the Ph.D. degree in electrical electromagnetics from Delft University of Technology, Delft, The Netherlands and with the Radar Department, Netherlands Organization for Applied Scientific Research (TNO) Defense, Safety and Security, The Hague, The Netherlands in 2020. She was a Post-Doctoral Researcher with the University of Siena, Siena, Italy from 2020 to 2021, and with the Public University of Navarra from 2021 to 2022. In 2022 she received the Post-Doctoral fellowship 'Juan de la Cierva' at the Public University of Navarra. Since 2022, she is an Antenna Scientist Innovator with the Antenna Group, Netherlands Organization for Applied Scientific Research (TNO) Defense, Safety and Security, The Hague, The Netherlands. She is the treasurer and secretary of the European School of Antennas and Propagation (ESoA) under the umbrella of EurAAP, and a member of the committee of the IEEE AP-S Young Professionals. Her current research interests include analysis and design techniques for phased array antennas and frequency-selective surfaces, analytical and numerical methods for antenna characterization, metasurfaces and metalenses. Dr. Yepes was a co-recipient of the Best Innovative Paper Prize at the 39th ESA Antenna Workshop in 2018.



Enrica Martini (S'98-M'02-SM'13) was born in Spilimbergo (PN), Italy, in 1973. In 1998, she received the Laurea degree (cum laude) in telecommunication engineering from the University of Florence, Italy, where she worked under a one-year research grant from the Alenia Aerospazio Company, Rome, Italy, until 1999. In 2002, she received the PhD degree in informatics and telecommunications from the University of Florence and the Ph.D. degree in electronics from the University of Nice-Sophia Antipolis, under joint supervision. In 2002, she was appointed Research Associate at the University of Siena, Italy. In 2005, she received the Hans Christian Ørsted Postdoctoral Fellowship from the Technical University

of Denmark, Lyngby, Denmark, and she joined the Electromagnetic Systems Section of the Ørsted•DTU Department until 2007. From 2007 to 2017 she was a Postdoctoral Fellow at the University of Siena, Italy. From 2016 to 2018 she was the CEO of the start-up Wave Up Srl, Siena, Italy, that she co-founded in 2012. She is currently associate professor at the University of Siena, Italy. She was the General Chair of the 16th International Congress on Artificial Materials for Novel Wave Phenomena (Metamaterials 2022). Dr. Martini was a co-recipient of the 2016 Schelkunoff Transactions Prize Paper Award, of the Best Paper Award in Antenna Design and Applications at the 11th European Conference on Antennas and Propagation in 2017, of the Best Poster Award at the Metamaterials Congress in 2019 and of the Best Paper Award in Electromagnetics at the 15th European Conference on Antennas and Propagation in 2021. Her research interests include metasurfaces, metamaterial characterization, electromagnetic scattering, antenna measurements, finite element methods and tropospheric propagation.



Stefano Maci (F'04) received the Laurea Degree cum Laude at University of Florence in '87 and from '97 is a Professor at the University of Siena. Since 2000, he was member the Technical Advisory Board of 16 international conferences and member of the Review Board of 6 International Journals. In 2004-2007 he was WP leader of the Antenna Center of Excellence (ACE, FP6-

EU) and in 2007-2010 he was International Coordinator of a 24-institution consortium of a Marie Curie Action (FP6). In 2004 he was the founder of the European School of Antennas (ESoA), a post graduate school that presently comprises 34 courses on Antennas, Propagation, Electromagnetic Theory, and Computational Electromagnetics and 150 teachers coming from 15 countries. Since 2004 is the Director of ESoA. Professor Maci has been a former member of the AdCom of IEEE Antennas and Propagation Society (AP-S), associate editor of IEEE AP-Transaction, Chair of the Award Committee of IEEE AP-S, and member of the Board of Directors of the European Association on Antennas and Propagation (EurAAP). From 2008 to 2015 he has been Director of the PhD program in Information Engineering and Mathematics of University of Siena, and from 2013 to 2015 he was member of the first National Italian Committee for Qualification to Professor. He has been former member of the Antennas and Propagation Executive Board of the Institution of Engineering and Technology (IET, UK). He founded and has been former Director of the consortium FORESEEN, involving 48 European Institutions. He was the principal investigator of the Future Emerging Technology project "Nanoarchitectronics" of the 8th EU Framework program, and he is presently principal investigator of the EU program "Metamask". Since 2010 he has been Principal Investigator of 6 cooperative projects and University coordinator of about other 20 cooperative projects financed by European Space Agency. He was co-founder of 2 Spin-off Companies. He has been a Distinguished Lecturer of the IEEE Antennas and Propagation Society (AP-S), and EuRAAP distinguished lecturer in the ambassador program. He was recipient of the EurAAP Award in 2014, of the IEEE Schelkunoff Transaction Prize in 2016, of the Chen-To Tai Distinguished Educator award in 2016, and of the URSI Dellinger Gold Medal in 2020. He has been TPC Chair of the METAMATERIAL 2020 conference and Chairperson of EuCAP 2023. In the last ten years he has been invited 25 times as key-note speaker in international conferences. He is the President of the IEEE Antennas and Propagation Society 2023. The research interest of Prof Maci includes high-frequency and beam representation methods, computational electromagnetics, large phased arrays, planar antennas, reflector antennas and feeds, metamaterials and metasurfaces. His research activity is documented in 200 papers published in international journals, (among which 100 on IEEE journals), 14 book chapters, and about 500 papers in proceedings of international conferences.